DOI: 10.1002/cphc.201000183

Evaluation of the Chemical Reactions from Two Electrogenerated Species in Picoliter Volumes by Scanning Electrochemical Microscopy

Qian Wang, Joaquín Rodríguez-López, and Allen J. Bard*[a]

The volume created by the positioning of two scanning electrochemical microscope (SECM) probes (tip and substrate) at a micrometric distance defines a "picoliter beaker" where homogeneous electron-transfer reactions are studied. The SECM is used to concurrently electrogenerate in situ two reactive species and to evaluate the possibility of detecting their reactivity. Two reaction cases are studied: the first, called the "reversible case", occurs when the electrochemically generated species at the substrate electrode can also react at the tip to yield the same product as the reaction in the gap. The second case, named the "irreversible case", occurs when the electrochemically generated species at the substrate are not able to react at the tip. Digital simulations are performed and compared to experimental studies. These show that an unusual compensation between collection and feedback effects render the analysis inapplicable in the "reversible case". The "irreversible case" is shown experimentally.

Introduction

Since its introduction about 20 years ago,[1,2] the scanning electrochemical microscope (SECM) has been used to study a variety of systems, both chemical and electrochemical;[3,4] these, however, have largely been confined to the study of surface reactivity and characterization of topography and to surface-bound chemical or biochemical systems.[1] Herein, we deal with the evaluation of the SECM as a tool to study chemical reactivity in a homogeneous phase, specifically electron-transfer reactions, where the reactants can be produced in situ through an electrochemical assembly in the picoliter volume created by positioning two ultramicroelectrodes (UME) at short distances.

The feedback mode of SECM consists in the monitoring of the current at a probe electrode (tip) when it interacts with a substrate.[1] The origin of this current is the electrogeneration of a reduced or oxidized species in solution by reduction or oxidation of a redox mediator at the tip. Measurable effects on this electrochemical signal are only possible when the probe and the substrate are close to each other, for example, to a distance shorter than about five times the UME radius where their diffusion layers can interact; a typical UME has a radius close to 10 μm or smaller. The electrogenerated species may be reactive towards chemical species at the substrate; thus, the feedback mode has been applied to study the heterogeneous reactivity, for instance, from mediators that "micro titrate" chemisorbed species at electrodes,[5,6] that chemically etch metals[7] involved in the study of the effects of mediator surface diffusion,[8–10] lateral charge propagation in polymer films,[11,12] and diffusion in monolayers,[13] as well as used in the detection of reactive species in living cells.[14] In these examples, the SECM probe acts both as a generator of the reactive species and as a transducing element as the feedback current indicates the existence and extent of chemical reaction.

Herein, we sought to find an analogy to the probing of surfaces with the evaluation of reactions in solution. One SECM approach to studying homogeneous electron-transfer reactions would take advantage of creating small reaction volumes at which feedback effects could be used to study the chemical reactivity of two electrogenerated substances in situ. A "picoliter beaker" is indeed a necessary condition for the SECM setup to concurrently generate the reactants and detect their reactivity, just as a small distance to the substrate is necessary in probe–surface feedback experiments. Figure 1 shows a schematic oversimplified view of such a setup in which two SECM probes (one of them acting as a tip and another as a substrate),[7] with embedded metal discs of radius a, are co-aligned and separated at a distance d. The tip and the substrate can generate reactive species which will react mainly in the volume defined by the interelectrode gap d and the extension of the flat end of the UMEs; this flat end is typically described by the dimensionless number RG which is obtained by dividing the radius of the tip's metallic disk including the insulating sheath of glass, rg, by the radius of the metallic disk, that is, $RG = rg/a$. The volume enclosed by these quantities can be imagined approximately as a cylinder, as shown in Figure 1. For a "large

[a] Q. Wang,[+] J. Rodríguez-López, Prof. Dr. A. J. Bard
Center for Electrochemistry
Department of Chemistry and Biochemistry
The University of Texas at Austin
Austin, TX 78712 (USA)
Fax: (+1) 512-471-0088
E-mail: ajbard@mail.utexas.edu

[+] On leave from Key Laboratory of Cluster Science
(Beijing Institute of Technology), Ministry of Education of China
Beijing, 100081 (China)

Supporting information for this article is available on the WWW under http://dx.doi.org/10.1002/cphc.201000183.

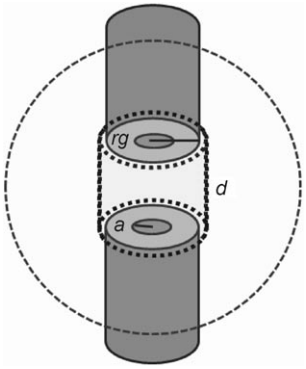

Figure 1. Schematic representation of the picoliter volume created by positioning two SECM probes at a distance *d*. The volume can be estimated by considering the inter-electrode gap, *d*, and the radius of the tip including the insulating sheath of glass, *rg*, such that $V \approx \pi rg^2 d$.

beaker" with $d \approx 50$ μm and UME's with radius $a \approx 10$ μm and $RG = 4$, the volume is estimated to be $V \approx 250$ pL. It will typically be smaller than this figure, for instance, $V \approx 25$ pL if $d \approx 20$ μm and $RG \approx 2$ with $a \approx 10$ μm, which are more common conditions for a two-electrode assembly. Strictly speaking, a larger volume needs to be considered to fully describe the system (large circle in Figure 1); however, the cylindrical pL volume suffices to describe most of the reaction front.

While a variety of experimental techniques and theoretical approaches exist for the study of homogeneous electron transfer,[15,16] we sought to evaluate the applicability of the SECM for the following main reasons: First, the versatility offered in general by electrochemistry[17] to generate coulometrically reactive species in situ at an electrode starting from unreactive parent molecules and without the necessary addition of chemical oxidants or reducing agents. Related to this, no isolation steps are required for the reactants since they can be produced directly in the reaction medium. In the case of relatively unstable molecules, at the micrometer sized tip–substrate gaps used in SECM (1–100 μm), molecules with lifetimes (based on first-order kinetic decomposition) on the order of 10–0.001 s can be studied by judicious choice of a controllable parameter, such as the distance between the SECM probes. Finally, the possibility of carrying out experiments at steady state and in which the SECM probe acts both as the reactant generator and reactivity detector simplifies notably the experimental design for the study of fast kinetics.[1]

The use of electrochemical methods for the study of following chemical processes, that is, homogeneous reactions that occur after electrochemical ones, has been extensively developed both experimentally and theoretically in the past 50 years,[17–19] especially for the case of cyclic voltammetry (CV). The use of the SECM in similar cases has already been explored and proved useful where mechanistic information, such as the rate of dimerization in organic[20] and biochemically relevant systems[21] or scavenging of reactive species[22] has been acquired using a combination of the tip generation–substrate collection (TG/SC) and feedback modes. Other SECM applications include the obtaining of kinetic parameters from electron-transfer reactions supported on the interface between two immiscible liquids,[23–25] and the use of following homogeneous reactions aimed at compressing the diffusion layer of SECM probes to increase their resolution, for example, for the patterning of materials[26] or the detection of biorelated analytes.[27]

The use of small volumes in the SECM, down to the zeptoliter mark, has been described before for the study of a small number of molecules;[28,29] it has been suggested in these SECM studies and in other submicron-fabricated electrochemical examples[30] that such platforms could be used to probe homogeneous reactions (and even individual reactions).[29] Although our picoliter approach is larger in dimensions, it perfectly allows the production of two reactants at different electrodes while using SECM feedback to evaluate their reactivity. Our intention is then to discuss the conditions under which this can be done and what type of information and applications can be envisioned.

Mode of Operation and Cases

The detection of reactivity in the "picoliter beaker" involves the use of feedback and generation/collection operation modes of SECM.[1] Two UME probes are used, both in the shape of SECM tips; we call one probe, the tip and the other the substrate, following usual SECM practice. The electrodes are aligned concentrically and the tip positioned at a fixed distance away from the substrate by the use of approach curves (i.e. current-to-distance relationships that apply for UMEs operating at steady state). The basic idea is to generate in situ a reactive species at each of the SECM probes, in this case an oxidized species at one electrode and a reduced species of a different redox couple at the other. The species diffuse away from the electrodes into the tip–substrate gap and react in a homogeneous electron transfer; the parent molecules do not react in their initial states, but are regenerated following the reaction of the electrogenerated species. This causes an increase in the diffusive flux of the parent molecules to their respective electrodes, which is reflected as an increase in the current measured at them; for practical purposes, from now on we refer to the increase in the tip current. The increase is similar to the one observed in the well-known feedback mode of SECM,[1,4] differing in the fact that it is brought about by a homogeneous reaction of the species in the tip–substrate gap rather than from regeneration through heterogeneous kinetics at the electrodes. Two general cases are treated, a "reversible" and an "irreversible" case, which are depicted in Figures 2 A and 2 B, respectively.

For the reversible case in Figure 2 A, two reversible mediators (a reducible species, O1, and an oxidizable species, R2, are initially present in the solution; O1 and R2 do not react, consistent with the current–potential (*I–E*) character of the system shown in Figure 2 panel A4. We now present a quick overview of the feedback and collection modes on the tip with this configuration with different potentials applied to tip and substrate. In Figure 1, panels A1 and A2, we show the usual SECM feedback cases where only one of the couples, either O1/R1 (A1) or O2/R2 (A2) are involved. In the feedback mode in A1,

the tip operates at a potential E_R, thus reducing O1 to R1 at a diffusion-limited rate, and the substrate is held at a potential E_M where it is unable to oxidize R2 to O2, but is able to oxidize R1 to O1. When this happens, the O1 that is fed back to the tip by diffusion causes an increased current at it, termed positive feedback. This increase in the tip current is only significant when the tip–substrate gap, *d*, is less than or about the radius of the tip microdisk, *a*. This implies that a narrow diffusion layer to which O1 is recycled and effectively recaptured by the tip is required for feedback.[1,2] Alternatively, in the tip collection mode for the O2/R2 couple, the tip is set at a potential E_M while the substrate is set to a potential E_O where it is able to oxidize R2 to O2 at a diffusion-limited rate. The tip in this case reduces O2 to R2 but is unable to reduce O1 to R1. Collection is a process that occurs over a much larger distance range than feedback, often spanning several tip radii with a detectable signal.[31]

The concept behind the methodology proposed here to study homogeneous electron transfer is to obtain a positive feedback-like response at the tip due to a second-order reaction of the tip-generated species with the substrate-generated species, as schematically shown in Figure 2, panel A3. In this experiment, the tip is set at a potential E_R while the substrate is set at a potential E_O. Reaction scheme 1 shows the relevant processes. Both electrodes are carrying out their respective reactions at a diffusion-limited rate and their products are being discharged mainly into the tip–substrate gap [Eqs. (1) and (2)] while the homogeneous reaction between the generated species proceeds according to Equation (3).

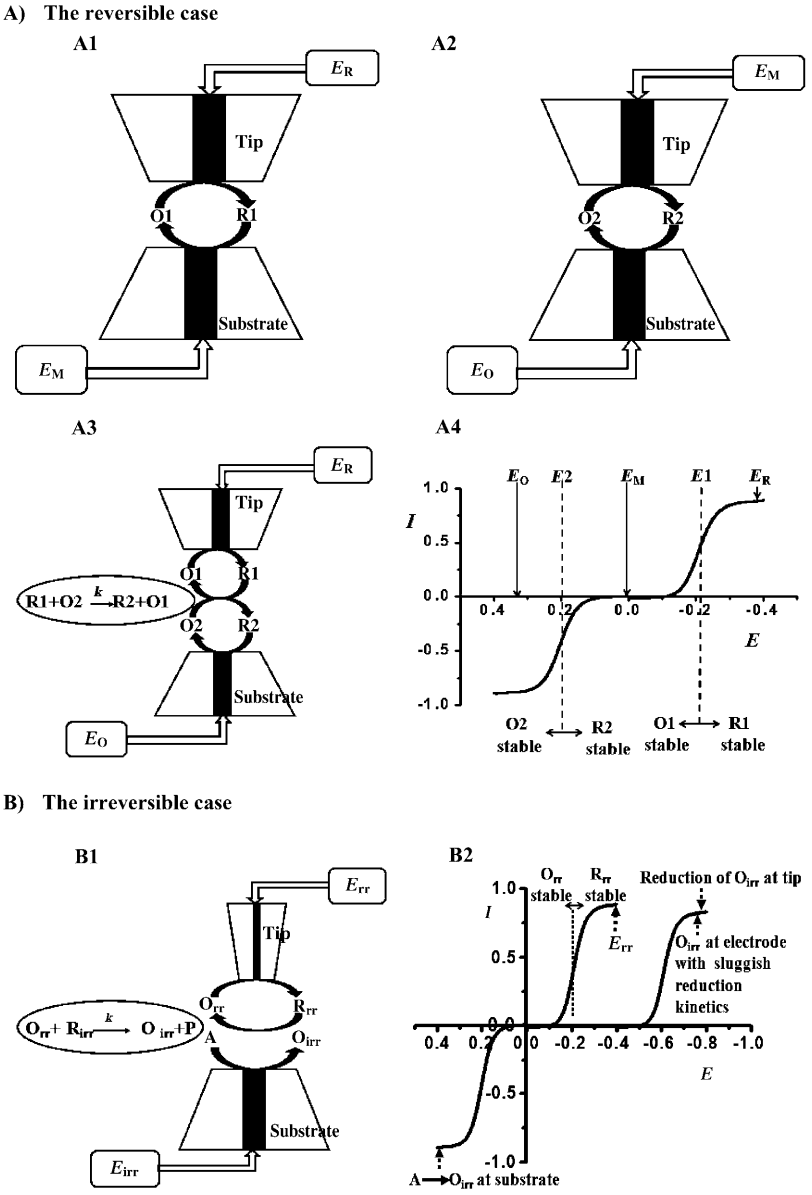

Figure 2. Schematics of the operation for the reversible (A) and irreversible case (B). A) Two electrochemically reversible mediators are used. A1) Feedback. The tip potential is set at the reduction potential (E_R) and the substrate held at the middle potential (E_M) such that positive feedback occurs by reaction of mediator 1. A2) Collection at the tip. The substrate is set at the oxidation potential (E_O) to oxidize mediator 2 while the tip is kept at E_M to reduce it back. A3) Annihilation in the gap. Tip is set at E_R to reduce mediator 1 and the substrate is set to E_O to oxidize mediator 2. The electrochemical products R1 and O2 react in the gap to regenerate O1 and R2. A4) *I–E* diagram of the potentials and predominant regions described. B) Electrochemically reversible behavior at the tip and generation of irreversible species at the substrate. The tip is unable to collect the species generated at the substrate. Electrode dimensions are explained further in the text. B1) Technique for the irreversible case. The tip reduces the reversible mediator (O_{rr} to R_{rr}) while the substrate generates a reducible species (O_{irr}). R_{rr} and O_{irr} react in the gap to regenerate O_{rr}. B2) *I–E* diagram showing the thermodynamic possibility of the irreversible case allowed by sluggish kinetics of the reaction of the irreversible species at the tip.

Reaction scheme 1:

$$O1 + e \rightarrow R1 \text{ heterogeneous, tip, diffusion limited} \quad (1)$$

$$R2 - e \rightarrow O2 \text{ heterogeneous, substrate, diffusion limited} \quad (2)$$

$$R1 + O2 \xrightarrow{k} O1 + R2 \text{ homogeneous, tip-substrate gap} \quad (3)$$

$$O2 + e \rightarrow R2 \text{ heterogeneous, tip, collection} \quad (4)$$

$$R1 - e \rightarrow O1 \text{ heterogeneous, substrate, collection} \quad (5)$$

The idea in reaction scheme 1 is that the production at the substrate of the reacting species O2, creates a regeneration boundary for O1 [Eq. (3)] that can serve in a similar way as the substrate electrode does to produce positive feedback, but at a closer distance than in the usual SECM case (compare panels A1 to A3 in Figure 2). Notice however that in this reversible system, Equations (4) and (5) in reaction scheme 1 predict a complication, because the tip and the substrate are concurrently set to a potential where they are able to consume the reactants in Equation (3). This also provides an electrochemical response at the tip of the same sign as the one expected for the effect of homogeneous reaction of R1 and O2. Unlike feedback and collection, the homogeneous reaction has fewer geometric restrictions, for example, the homogeneous electron transfer occurs in a volume, rather than on a surface. It should be possible to obtain, experimentally, a difference in the tip current when subtracting the maximum possible feedback (Figure 1, panel A1) and the maximum possible collection (Figure 1, panel A2), as shown in Equation (6):

$$i_{react} = i_{ann} - i_{feed} - i_{coll} \quad (6)$$

where i_{ann} stands for the current read by the tip during the annihilation [second-order reaction, Eq. (3)] experiment, i_{feed} stands for the current read during a positive feedback experiment, and i_{coll} stands for the current read during a collection experiment (of the substrate product). i_{react} stands then for a distinguishable current that would depend on the kinetics of the electron-transfer reaction, accessible by the use of digital simulations, which have been successfully used to characterize diverse SECM systems.[1] The reversible case was studied experimentally by the probing of the reaction between electrogenerated $Fe(CN)_6^{3-}$ and $Ru(NH_3)_6^{2+}$ from their precursors (see Experimental Section).

The irreversible case, as shown in Figure 2B, avoids the collection complication outlined previously. Here, a reversible mediator (O_{rr}/R_{rr}, equivalent to O1/R1) is again used at the tip, generating R_{rr} by reduction of O_{rr}, and a chemically irreversible species O_{irr} is generated at the substrate from an inactive species A (Figure 2, panel B1). Electrochemical reduction of O_{irr} is assumed to occur only at an electrocatalytic electrode. Thermodynamically, the reaction between R_{rr} and O_{irr} in the tip–substrate gap is allowed, however, the electrochemical reduction of O_{irr} at the tip is prevented by choosing a tip material that lacks the catalytic properties required to reduce O_{irr}. As shown in Figure 2, *I–E* diagram in panel B2, the tip is able to reversibly act on the O_{rr}/R_{rr} pair; however, it requires a substantial overpotential to be able to react O_{irr}. Reaction scheme 2 summarizes the behavior of this system.

Reaction scheme 2:

$$O_{rr} + e \rightarrow R_{rr} \text{ heterogeneous, tip, diffusion limited} \quad (7)$$

$$A - e \rightarrow O_{irr} \text{ heterogeneous, substrate} \quad (8)$$

$$R_{rr} + O_{irr} \rightarrow O_{rr} + P \text{ homogeneous, tip} - \text{substrate gap} \quad (9)$$

$$R_{rr} - e \xrightarrow{k} O_{rr} \text{ heterogeneous, substrate, collection} \quad (10)$$

$$O_{irr} + e \xrightarrow{x} \text{A tip, allowed only if catalytic} \quad (11)$$

When Equation (11) applies by inhibiting the collection of O_{irr} at the tip, Equation (6) simplifies to Equation (12):

$$i_{react} = i_{ann} - i_{feed} \quad (12)$$

Because of the additional constraints presented by the irreversible mechanism, the selection of a suitable system to prove this case is more difficult and consequently the direct characterization of i_{react} is probably less straightforward. We discuss the reduction of electrogenerated O_2 (acting as O_{irr}, and generated from the platinum-catalyzed oxidation of H_2O) by Fe^{II}[EDTA] (generated at the tip from Fe^{III}[EDTA]) to produce the final product H_2O[32–34] and regenerating the initially present Fe^{III}[EDTA]. For this purpose, a combined SECM study and the direct use of digital simulations allows for a much easier understanding of the described irreversible system.

Digital Simulations

The diffusion and kinetic problem was simulated using the finite element method provided by the Comsol Multiphysics v.3.2 software (COMSOL, Inc., Burlington, MA) in axial 2D symmetry (variables are *r, z*) under steady-state conditions. A complete report on the simulation can be found in the Supporting Information.

The Reversible System

The geometry of the problem was assumed to be the one presented in Figure 2A and diffusion and kinetic conditions as outlined in reaction scheme 1. Equations (1), (2), (4), and (5) are assumed to occur at the electrodes at a diffusion-limited rate at both the tip and the substrate (at the inlaid electrode boundary); the potentials were recreated as in Figure 2A, panel A3, with the tip potential set at E_R and the substrate at E_O. The flux J to the electrodes, which is coupled to diffusion and kinetics in the inter-electrode gap, was modelled using Butler–Volmer conditions, Equations (13) and (14) for each pair of species, and assumed for both reactions a standard rate constant $k^0 = 0.1\ m\,s^{-1}$ and a transfer coefficient $\alpha = 0.5$; $f = 38.94\ V^{-1}$. Equations (13) and (14) are used to describe the flux of each species to the tip; in the case of the substrate, E_R is replaced by E_O (see Equations S2 and S3 of the Supporting Information). The following parameters were chosen for the potentials: $E_R = -0.4$ V, $E_O = 0.4$ V and formal potentials $E^{0'}{}_1 = -0.2$ V for the O1/R1 pair and $E^{0'}{}_2 = 0.2$ V for the O2/R2 pair; this ensured the recreation of the predominant regions and the *I–E* characteristics shown in Figure 2A, panel A4. We also assumed that the diffusion coefficients of the members in each redox pair were the same. Under these conditions, the electrodes exhibit the typical response for a system with positive feedback and collection [Eqs. (13) and (14)]:

$$J_{O1} = k^0 (C_{O1,s} e^{-\alpha f (E_R - E^{0'}_1)} - C_{R1,s} e^{(1-\alpha) f (E_R - E^{0'}_1)}); \; J_{R1} = -J_{O1} \quad (13)$$

$$J_{O2} = k^0(C_{O2,s}e^{-\alpha f(E_R - E_2^{0'})} - C_{R2,s}e^{(1-\alpha)f(E_R - E_2^{0'})}); J_{R2} = -J_{O2} \quad (14)$$

In Equations (13) and (14), $C_{O1,s}$, $C_{O2,s}$, $C_{R1,s}$ and $C_{R2,s}$ represent the concentrations of the species at the electrode boundary (either tip or substrate) and are determined by the coupling of the diffusive and kinetic problem. As an initial condition, only O1 and R2 are present in the simulation subdomain and have bulk concentrations $C_{O1}^* = C_{R2}^* = 1$ mM. The diffusion problem is coupled to the homogeneous kinetics at the tip–substrate gap, which is represented by Equation (3) and solved at steady state for different values of the reaction constant k. For the tip electrode ($z = 0$), it is possible in the simulations to separate the electrochemical response (given as the integral of the flux of a given species at the microdisk boundary) due to feedback of the O1/R1 pair [Eq. (15)] and the collection of O2 [Eq. (16)]:

$$i_{(feed+ann)} = \int_{r=0}^{r=a} 2\pi nFDr\frac{\partial C_{O1}(r,0)}{\partial z}dr \quad (15)$$

$$i_{coll} = \int_{r=0}^{r=a} 2\pi nFDr\frac{\partial C_{O2}(r,0)}{\partial z}dr \quad (16)$$

In Equations (15) and (16), n stands for the number of exchanged electrons, F is Faraday's constant (96485 C mol^{-1}), a is the radius of the microdisk electrode, and D stands for the diffusion coefficient of the species.

The Irreversible Case

For this case, the experimental geometry that is sketched in Figure 2B was used. Butler–Volmer kinetics are used to model the flux boundary condition at the electrode surfaces for the reversible redox mediator O_{rr}/R_{rr} (E_R is used at the tip and E_O at the substrate), for example, Equation (17) for the tip. The generation of the irreversible species, O_{irr}, is recreated by using a concentration boundary condition at the substrate [Eq. (18)] and the tip shows no reactivity towards this species (insulating boundary):

$$J_{Orr} = k^0(C_{Orr,s}e^{-\alpha f(E_R - E_{rr}^{0'})} - C_{Rrr,s}e^{(1-\alpha)f(E_R - E_{rr}^{0'})}); J_{Rrr} = -J_{Orr} \quad (17)$$

$$C_{Oirr} = c \quad (18)$$

In Equation (17), the following parameters were chosen: $E^{0'}_{rr} = 0$ V, $E_R = -0.2$ V ($E_O = 0.2$ for the substrate), $k^0 = 0.1$ m s^{-1}, and $\alpha = 0.5$; $C_{Orr,s}$ and $C_{Rrr,s}$ represent the concentrations of O_{rr} and R_{rr}, respectively, at the surface of the electrode. In Equation (18), c is a fixed concentration value that is used as a consequence that the reaction to generate C_{Oirr} is not diffusion-limited; nonetheless, it is operating at steady state. The homogeneous electron transfer is considered to proceed through Equation (9), although in the system studied, that is, the reduction of O_2 (O_{irr}) by Fe^{II}[EDTA] (R_{rr}) four sequential processes—each involving a molecule of Fe^{II}[EDTA]—were taken into account to model the four electron transfers to complete the reduction of O_2 to H_2O. The first step was considered to be rate-determining and the following three steps were modeled to be close to diffusion control.

Due to the lack of electrochemistry of O_{irr} at the tip, the electrochemical response at the tip is simply obtained by Equation (19):

$$i_{(feed+ann)} = \int_{r=0}^{r=a} 2\pi nFDr\frac{\partial C_{Orr}(r,0)}{\partial z}dr \quad (19)$$

An additional procedure that had to be taken into account to model the irreversible case was the determination of the concentration c in Equation (18). This was done in an independent collection experiment where two platinum SECM tips were aligned concentrically and one of them generated O_2 that was collected by the other. The equivalent concentration of oxygen produced at the substrate was obtained through simulation and the value fed to the annihilation simulations discussed above. Details are given in the Supporting Information.

Experimental Section

Chemicals: All chemicals were used as received. Potassium sulfate (K_2SO_4, Aldrich, St. Louis, MO), potassium ferrocyanide ($K_4Fe(CN)_6 \cdot 3H_2O$), A.C.S reagent), hexaammineruthenium(III) chloride (99%, $[Ru(NH_3)_6]Cl_3$, Strem Chemicals, Newburyport, MA), agar (Purified grade), sodium perchlorate (99%, $NaClO_4$, A.C.S reagent). All solutions were prepared with deionized Milli-Q water. Acetate buffer solution (pH 4.7) was prepared by adjusting the pH of a 0.3 M solution of sodium acetate ($NaC_2H_3O_2$, Fisher scientific,A.C.S reagent) with acetic acid ($C_2H_4O_2$, Fisher Scientific, A.C.S reagent). Fe^{III}[EDTA] solution was prepared by dissolution of iron(III) nitrate nonahydrate (98%, $Fe(NO_3)_3 \cdot 9H_2O$, Aldrich, A.C.S reagent) and (Ethylenedinitrilo)- tetraacetic acid, disodium salt dihydrate ($Na_2H_2EDTA \cdot 2H_2O$, A.C.S reagent) in 0.3 M acetate buffer solution (pH 4.7).

Solutions were bubbled with humid Ar prior to any electrochemical experiment and kept under the Ar blanket during experiments.

Electrodes: The SECM tips were fabricated using gold (99.99%) or platinum (99.99%) wires (25 μm in diameter) from Goodfellow (Devon, PA), sealed in soft glass by procedures described elsewhere.[1] A carbon fiber tip was fabricated by the same procedure using carbon yarn (10 μm in diameter, Alfa-Aesar, Newburyport, MA). All electrodes were polished on microcloth pads (Buehler, Lake Bluff, IL) with alumina paste (0.05 μm) and then sonicated for 15 min in deionized Milli-Q water prior to use. The platinum electrodes had an $RG = 5$ and gold electrodes had an $RG = 4$ while the carbon fiber tip had an $RG = 10$, where $RG = r_g/a$, r_g being the radius of the glass insulating layer around the microdisk, including the radius of the microdisk itself.

A Ag/AgCl in saturated KCl reference electrode and a 1 M sodium perchlorate 3% w/v agar gel salt bridge (to avoid excessive chloride contamination from leakage through the glass frit of the reference) were used for all the experiments. All potentials in this study are referred to the Ag/AgCl (saturated KCl) electrode. A piece of 0.5 mm tungsten wire from Alfa (Danvers, MA) was used as the counter electrode in all experiments. All electrochemical measurements were performed using either a CHI900 or a CHI920C SECM (CH Instruments, Austin, TX).

Experimental Procedure: Both tip and substrate are UMEs for the electrode setup. The substrate was fixed in a Teflon electrochemi-

cal cell by inserting it through a drilled hole at the bottom of the cell and the tip was positioned roughly above it. The solution was then introduced and a mediator used first to find the position of the substrate electrode by the tip generation–substrate collection mode, which is more sensitive over longer distances. The tip and substrate were then aligned concentrically by the use of approach curves and X and Y scans, as described elsewhere.[5]

The Reversible Case: We take the reaction of $Fe(CN)_6^{3-}$ and $Ru(NH_3)_6^{2+}$, generated from the precursors $Fe(CN)_6^{4-}$ and $Ru(NH_3)_6^{3+}$, as an example. Once the electrodes were aligned by use of either redox pair $[Fe(CN)_6^{4-}/Fe(CN)_6^{3-}$, $E_{1/2}=0.24$ V vs. Ag/AgCl or $Ru(NH_3)_6^{3+}/Ru(NH_3)_6^{2+}$ $E_{1/2}=-0.19$ V vs. Ag/AgCl], the electrodes were withdrawn to an approximate distance of 200 μm and single mediator approach curves were obtained. Feedback and tip generation–substrate collection approach curves were recorded and used to calibrate the tip–substrate distance and to compare to other cases; these were obtained by setting the tip to a potential where diffusion-limited reduction of $Ru(NH_3)_6^{3+}$ to $Ru(NH_3)_6^{2+}$ ($E_{tip}=-0.4$ V vs. Ag/AgCl) was accomplished and the substrate set to a more positive potential ($E_{sub}=0$ V vs. Ag/AgCl) which is sufficient for the oxidation of $Ru(NH_3)_6^{2+}$, but still does not cause appreciable oxidation of $Fe(CN)_6^{4-}$. For the annihilation approach curves, the tip is held at a potential to reduce $Ru(NH_3)_6^{3+}$ to $Ru(NH_3)_6^{2+}$ ($E_{tip}=-0.4$ V vs. Ag/AgCl) and the substrate held at a potential to oxidize $Fe(CN)_6^{4-}$ to $Fe(CN)_6^{3-}$ ($E_{sub}=0.4$ V vs. Ag/AgCl). Additionally, measurements were taken at fixed distances between the tip and substrate; chronoamperograms were obtained at these same potentials and the average steady-state currents read after 30 s were used to apply Equation (6).

The Irreversible Case: We take as an example the reaction of electrogenerated O_2 (at a Pt substrate by oxidation of water) with Fe^{II}-[EDTA] electrogenerated at the tip from Fe^{III}[EDTA]. As a first step, a calibration experiment was run to determine the amount of oxygen discharged into the tip–substrate gap by the following procedure: Two Pt UME ($a=12.5$ μm, $RG=5$) were aligned concentrically and immersed in 0.3 M acetate buffer (pH 4.7), the distance between them was 20 μm. Substrate generation/tip collection was carried out using CV at the substrate and setting the Pt tip collector to a potential where diffusion-limited reduction of O_2 to water occurs ($E_{collector}=-0.1$ V vs. Ag/AgCl). The substrate was swept at a slow scan rate $(\nu=20\ mV\,s)^{-1}$ from 1.0 V to 1.8 V. The current read at the tip collector was used as the experimental parameter for digital simulations to determine the amount of oxygen available for reaction at selected substrate potentials for its use in the annihilation experiments. Following this, the setup described in Figure 1B was used. A carbon fiber tip was approached to and aligned with a Pt substrate using the positive feedback mode. The tip was set to a potential that allowed the diffusion controlled generation of Fe^{II}[EDTA] from Fe^{III}[EDTA] ($E_{tip}=-0.6$ V vs Ag/AgCl) and the substrate to a potential where the oxidation of Fe^{II}[EDTA] was possible without the discharge of any reactive product (i.e. oxygen) into the solution ($E_{sub}=0.2$ V vs Ag/AgCl). The tip was then set a desired distance away from the substrate and the annihilation experiment run. The tip was held at the diffusion-limited reduction of Fe^{III}[EDTA] while the substrate potential was scanned slowly ($\nu=20\ mV\,s^{-1}$) to over a range of potentials where the oxidation of water to O_2 is possible (from 1.0 to 1.8 V vs. Ag/AgCl).

Results and Discussion

The Reversible Case

For the reversible system, two Au UMEs ($a=12.5$ μm, $RG=4$) were used as tip and substrate, respectively. Two well-known mediators, $Fe(CN)_6^{4-/3-}$ and $Ru(NH_3)_6^{3+/2+}$, were selected to form the reversible system. A typical tip CV of a solution containing 1 mM $Fe(CN)_6^{4-}$ and 1 mM $Ru(NH_3)_6^{3+}$ is shown in Figure 3; these species exhibit a reversible behavior, and their UME voltammogram shows the characteristic sigmoid shape; the plateau limiting current (i_{ss}) is described by Equation (20):

$$i_{ss} = 4nFDac^* \qquad (20)$$

where n is the number of electrons, F is the Faraday constant, D is the diffusion coefficient of the mediator, a is the radius of the tip, and c^* is the bulk concentration of the species. For $Fe(CN)_6^{4-}$ and $Ru(NH_3)_6^{3+}$, the reported values of D are 7.2×10^{-6} and $5.5\times10^{-6}\ cm^2\,s^{-1}$, respectively;[35] these values are close enough that in the medium used for this case, the limiting current appears to be of essentially the same magnitude (Figure 3).

Figure 4A shows the usual single mediator approach curve in the feedback mode (using the $Ru(NH_3)_6^{3+/2+}$ pair) and the substrate current when the tip is set to a potential E_R and the substrate to a potential E_M according to Figure 2A. The tip and substrate currents (i_T and i_S) are normalized with respect to the steady-state tip current at infinite distance, $i_{T,\infty}$, and distances with respect to the radius of the tip, where $L=d/a$. The feedback at the tip and the collection at the substrate are shown to correspond very well to the simulation results as expected from this well-behaved mediator. Notice that as mentioned earlier in the mode of operation, collection spans a much larger distance than the change in the response brought by positive feedback. The expectation is that in the annihilation experiment, the reaction of the tip generated product with the diffusing species produced at the substrate will produce great-

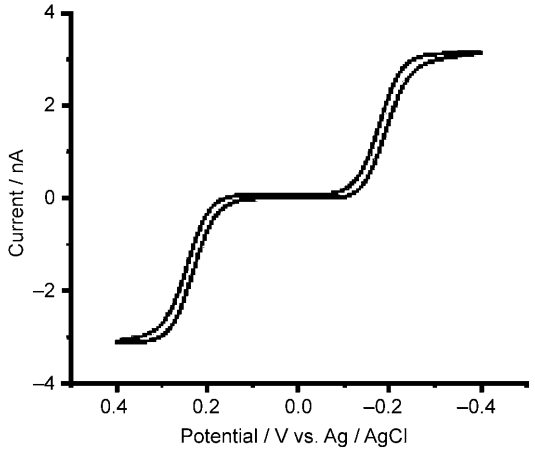

Figure 3. Typical CV of the reversible system. Tip: Au UME ($a=12.5$ μm, $RG=4$); Solution: 1 mM $Fe(CN)_6^{4-}$ and 1 mM $Ru(NH_3)_6^{3+}$ in 0.1 M K_2SO_4 purged with Ar, $\nu=20\ mV\,s^{-1}$.

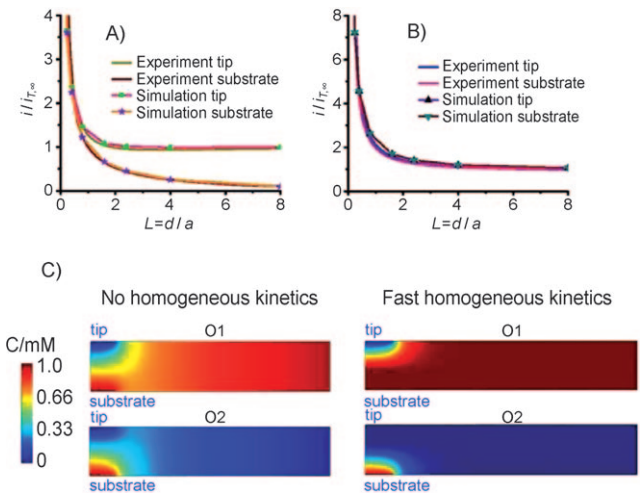

Figure 4. Experimental and simulated approach curves of the reversible system. Both tip and substrate are 12.5 μm in radius Au UMEs ($RG=4$). 1 mM $Fe(CN)_6^{4-}$ + 1 mM $Ru(NH_3)_6^{3+}$ solution in 0.1 M K_2SO_4 bubbled with humid Ar and kept under Ar blanket. Approach rate: 2 μm s^{-1}. A) Normal approach curve. Tip potential was applied at E_R ($E_{tip}=-0.4$ V vs. Ag/AgCl) and the substrate held at E_M ($E_{sub}=0$ V vs. Ag/AgCl). B) Annihilation approach curve. Tip held at E_R ($E_{tip}=-0.4$ V vs Ag/AgCl) and the substrate was kept at E_O ($E_{sub}=0.4$ V vs Ag/AgCl). C) Simulated concentration profiles for the species O1 and O2 when $k=0\ M^{-1}s^{-1}$ (left) and $k=1\times10^{10}\ M^{-1}s^{-1}$ (right). Space is zoomed-in into the tip–substrate gap. The locations of tip and substrate microdisks are indicated.; $d=20$ μm.

er feedback at a given d compared to the usual single mediator case. That is, the far reaching diffusion layer created by the discharge $Fe(CN)_6^{3-}$ and $Ru(NH_3)_6^{2+}$ will provide a closer reaction front to the tip from which an increased positive feedback-like response could be obtained. Thus, one might expect that the response would depend on the second order homogeneous electron transfer reaction constant, k, whose value could be determined by use of Equation (6) coupled to the results from digital simulations.

Figure 4B shows an annihilation approach curve in which now the tip is set at a potential E_R and the substrate at a potential E_O so that reactants $Fe(CN)_6^{3-}$ and $Ru(NH_3)_6^{2+}$ are produced and react in the same fashion as shown in Equation (3). The recorded currents show a clear increase in the electrochemical activity in the system, as evidenced by the nearly twofold increase in the normalized current at short distances (small L) while at larger distances the normalized current tends to unity. The result of the digital simulations however indicates an unexpected feature: *the current at the tip is the same for all values of the homogeneous rate constant, k*. This is the product of compensation between positive feedback, both coming from heterogeneous reaction at the substrate and from the homogeneous reaction in the gap, and collection of the substrate product at the tip. Figure 4B shows that the experimental data fits very well this k-independent electrochemical response. Figure 4C depicts the simulated behavior of the system when $k=0\ M^{-1}s^{-1}$ and when $k=1\times10^{10}\ M^{-1}s^{-1}$ (close to second-order diffusion-limited conditions) by showing the concentrations of O1 ($Ru(NH_3)_6^{3+}$), the species whose flux is responsible for providing the positive-feedback response at the tip, and of O2 ($Fe(CN)_6^{3-}$), the species responsible for the collection response at the same electrode. The figure shows a zoom-in into the tip–substrate gap region, and clearly evidences that the concentration profiles in both cases are very different. When there is a lack of reaction in the gap ($k=0$), O1 is recycled by virtue of heterogeneous reaction at the substrate and O2 is able to freely penetrate the diffusion layer of R1, to diffuse towards the tip, and to be collected.

In the case of high reaction kinetics ($k=10^{10}\ M^{-1}s^{-1}$), the interpenetration of O2 to the tip is almost zero and as hypothesized earlier, the reaction front due to homogeneous reaction (which is created halfway through the tip-substrate gap) lies closer to the tip. This contracts the diffusion layer of O1 at the tip and gives an increase in the feedback response at the expense of losing the collection that would otherwise be present, although in the same amount. Table 1 summarizes a balance sheet example of this effect.

Table 1. Balance sheet from digital simulation results showing the contribution of feedback and collection to the current read at the tip.

No reaction kinetics $k=0\ M^{-1}s^{-1}$		High reaction kinetics $k=1\times10^{10}\ M^{-1}s^{-1}$	
***d*=50 μm**		***d*=50 μm**	
Feedback	2.3259×10^{-9} A	Feedback	2.9254×10^{-9} A
Collection	0.5994×10^{-9} A	Collection	9×10^{-20} A
Total current	2.9253×10^{-9} A	Total current	2.9254×10^{-9} A
***d*=20 μm**		***d*=20 μm**	
Feedback	2.5512×10^{-9} A	Feedback	4.1121×10^{-9} A
Collection	1.5610×10^{-9} A	Collection	1×10^{-14} A
Total current	4.1122×10^{-9} A	Total current	4.1121×10^{-9} A

The results shown in Table 1 depict the compensation effect that the loss of collection and gain in feedback create when going from a non-reactive system (left panel, Table 1), to a reactive one (right panel, Table 1) with equal diffusion coefficients. Small differences in the fourth significant figure (sub-picoampere level) do occur; however, they are experimentally inaccessible in this situation, and may be assignable to simulation error. As mentioned previously, the simulation allows us to separate the feedback from the collection response; however, experimentally this is not possible and it is necessary to go to Equation (6). To do so, we performed experiments at different values of d, in which the feedback (Figure 2, panel A1), collection (Figure 2, panel A2), and annihilation (Figure 2, panel A3) responses acquired through chronoamperometry at steady state were applied to Equation (6). Figure 5 shows representative results of this operation in which the experimental i_{react} [defined in Eq. (6)] is plotted against the tip–substrate distance d; except for a less reproducible point at $d=5$ μm, the value of i_{react} is in the 10^{-11}–10^{-12} A range.

Experimentally, it would be difficult to expect the same differences predicted by the simulation, and it is possible that small effects created by less controllable effects, such as convection, may be responsible for i_{react} to be in this current range. In the case of the result at shorter distance, it is possible that steady-state[8,36] or transient[5] surface phenomena are responsible for the larger differences observed. The experimental re-

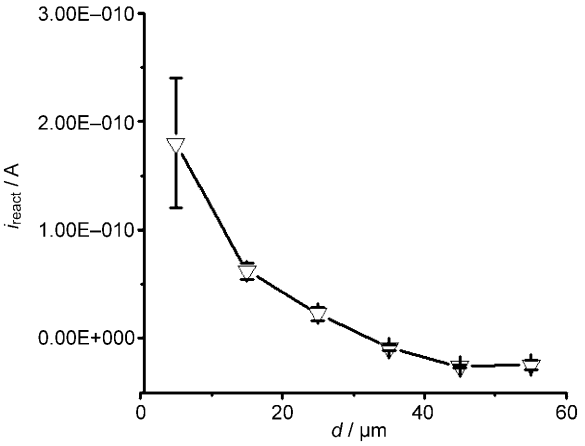

Figure 5. Experimental i_{react} versus tip–substrate distance, *d*, including error bars for three measurements.

sults agreed well, within the experimental error, with the simulated prediction. Additional experiments done with other redox systems (see Supporting Information, Figures S1 and S2) seem to confirm this compensation effect. Moreover, other experimental strategies such as changing the symmetry of the SECM system by displacing the tip with respect to the substrate in the *X* or *Y* axis (see Supporting Information, Figure S3) or by changing the *RG* of the tip and/or substrate, did not produce significant differences in i_{react}. Other strategies for studying this case are under way in our group in which the use of a coupled technique such as electrogenerated chemiluminescence (ECL) may yield some information about similar schemes in the case of highly exergonic reactions.[37] In this case, the annihilation reaction can be demonstrated because light emission is an indicator of chemical reactivity and because the distribution of such emission can be studied spatially, for example, at different distances between the generating electrodes,[37] or by optical sampling of the spatial emission profile.[38]

The Irreversible Case

Since the compensation effect on the tip response shown for the reversible case originates from the changes in the collection of the substrate generated species, the elimination of the collection channel should yield a distinguishable change in the feedback response. This can be accomplished by using an irreversible reaction at the substrate, where the tip cannot collect the substrate generated species, because it does not react (for kinetic reasons) at potentials where the reversible mediator is generated. In such an example, the reduced mediator can react with the substrate-generated oxidant and acts as a catalyst for the ET. A model reaction between Fe^{II}[EDTA] (generated from Fe^{III}[EDTA] at the tip) and O_2 (evolved from water at a Pt substrate) was used. The kinetics of this system have been reported and its complex mechanism studied and compared under a variety of conditions.[39] Our motivation here is to demonstrate the feasibility of the irreversible case through the observation of the reactivity of the electrogenerated species through the SECM technique rather than to provide detailed mechanistic information about the reaction. The oxygen reduction reaction (ORR) is a multi-step complicated reaction; the complete reduction of oxygen to water involves the transfer of four electrons and four protons, with cleavage of the O–O bond, where the intermediate electron transfer events can yield different products (such as hydrogen peroxide) and depends on factors like the solution composition (pH, ionic force, reducing agent)[32–34,40] or electrode material and electrode potential in the case of electrochemical reduction.[31,39,41] Under the conditions used in this study, the succeeding electron-transfer steps have been reported to be fast ($k = 1 \times 10^{10}$ M^{-1} s^{-1}).[42] The reaction is assumed to proceed in four elementary steps that yield the overall reaction shown in Equation (21):

$$4\,Fe^{II}[EDTA] + O_2 + 4\,H^+ \rightarrow 4Fe^{III}[EDTA] + 2\,H_2O \qquad (21)$$

At high positive potentials, ($E >$ 1.2 V vs. Ag/AgCl), oxygen is evolved from the Pt substrate according to Equation (8), where A is water and O_{irr} is oxygen. The amount of O_2 generated at the substrate as a function of oxidation potential and at steady-state conditions was calibrated by a collection experiment in which a Pt SECM tip was used as the probe. The collection data was fed to the digital simulations to find the concentration boundary condition to be used later on. The conditions were maintained so that gaseous O_2 was not evolved. At more positive potentials the current density increased and more oxygen was produced at steady state; in the potential range used at the Pt substrate, the determined oxygen concentrations were below 0.5 mM, approximately its saturation limit in the aqueous solvent.

To make sure oxygen was reduced by Fe^{II}[EDTA] and not by the tip, a carbon fiber UME was used; this material requires a considerable overpotential to activate the electroreduction of O_2, and furthermore, it is relatively inactive in acidic solutions towards the reduction of intermediate species such as hydrogen peroxide.[43] Figure 6 shows the CV at the carbon tip for reduction of Fe^{III}[EDTA] to Fe^{II}[EDTA], which occurs at less positive potentials than the reduction of oxygen, as shown in the inset of Figure 6 (this is analogous to the case in Figure 2, panel B2). Despite the capacitive nature of the CV in Figure 6, which is typical of high roughness carbon tips, a very stable steady-state response was obtained ($i_{ss} = 0.9$ nA at -0.5 V vs. Ag/AgCl) and by use of Equation (20), we calculate the diffusion coefficient of Fe^{III}[EDTA] to be $D = 4.6 \times 10^{-6}$ cm^2 s^{-1} which is consistent with reported values.[44]

Once the carbon tip and the substrate were aligned, the annihilation experiment was run with a fixed distance $d = 20$ μm. The reaction rate was controlled by selection of the substrate potential (which determines the amount of oxygen produced). The tip potential was kept at -0.5 V, where Fe^{III}[EDTA] can be reduced to Fe^{II}[EDTA] and O_2 is not reduced, while the substrate was scanned slowly ($\nu = 20$ mV s)$^{-1}$ from 1.0 to 1.7 V to generate O_2. Figure 7 A shows the Pt tip collection curve obtained from the calibration experiment to determine the equivalent O_2 concentrations at the substrate (see Supporting Information, Table 1) while Figure 7 B shows the carbon tip re-

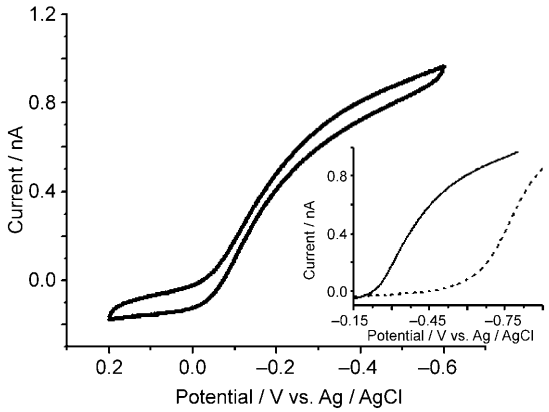

Figure 6. Carbon fiber tip ($a = 5$ μm, $RG = 10$) CV of 1 mM Fe^{III}[EDTA] in 0.3 M acetate buffer (pH 4.7) solution without O_2. Scan rate: 10 mV s^{-1}. The inset shows a comparison of the forward scan for the reduction of Fe^{III}[EDTA] (——) with the background-subtracted forward scan for the reduction of O_2 at the same tip in an air-saturated solution without Fe^{III}[EDTA] (•••••).

sponse with the Fe^{III}[EDTA] mediator during the annihilation experiment. In Figure 7B, as the concentration of O_2 available in the tip–substrate gap increases, the tip current also increases, in line with an increase in the reaction rate, as depicted in Equations (9) and (21). Provided that the tip is only responsive to the flux of Fe^{III}[EDTA], the species that undergoes regeneration in each reaction step, the increased positive feedback-like response is a reflection of the rate of the reaction in the gap. Figure 7B also shows a comparison to the simulated results, in which the first electron transfer (out of four, as mentioned above, and represented by k_1) is taken as rate-determining. The following three electron-transfer steps are assumed to be close to diffusion-limited conditions ($k_2 = k_3 = k_4 = 1 \times 10^9$ M $^{-1}$ s^{-1}). The simulations also indicate that the increase in the tip current is indeed due to the same effect of compression of the diffusion layer of the reversible mediator, as was discussed for the reversible case (Figure 4C). The tip response, as shown in Figure 7B, is at the high end of the accessible bimolecular rate constants measurable by this technique; note also that the tip current fits well the maximum response predicted at various simulated substrate potentials. At more positive potentials, the deviations observed both in the collection experiment and the annihilation experiment may be due to the discharge of other reaction species that are not taken into account in the simulation, such as O_3 or Pt^{2+} (from the anodic dissolution of Pt). The comparison made in Figure 7B also allows us to estimate a working range of rate constants of about four orders of magnitude that can be distinguished clearly. At this distance, a working range of 10^3 M $^{-1}$ $s^{-1} < k_1 < 10^7$ M $^{-1}$ s^{-1} was estimated. It is possible that modest increases in this working range could be accessed by judicious selection of the tip–substrate distance; however, much smaller gaps that could lead to quantification of much larger rate constants would be technically challenging, while larger distances to quantify smaller rate constants would be accompanied by a decrease in the feedback signal. In this case, the size of the "picoliter beaker" determines also the quality and type of information that can be obtained from the experiment.

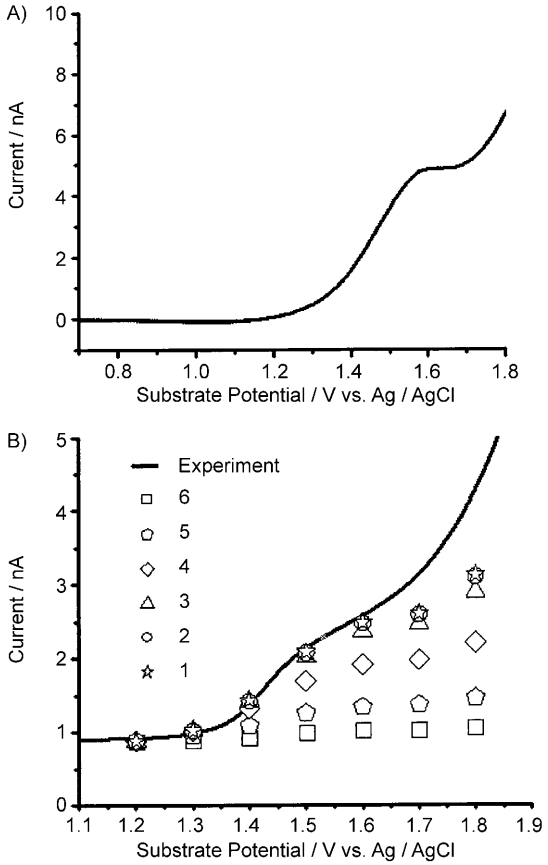

Figure 7. Results of the irreversible system. All the solutions were bubbled with humid Ar and kept under Ar blanket. A) Pt tip current of calibration for oxygen evolution on a Pt substrate. Both generator and collector, $a = 12.5$ μm, $RG = 5$. Solution: 0.3 M acetate buffer, pH 4.7 (the approximate buffer capacity is 0.15 M). B) Tip current including the response due to homogeneous electron transfer between oxygen generated at the substrate and Fe^{II}[EDTA] generated at the tip. Tip: Carbon fiber UME ($a = 5$ μm, RG = 10). Substrate: Pt UME ($a = 12.5$ μm, RG = 5). Solution: 1 mM Fe^{III}[EDTA] in 0.3 M acetate buffer (pH 4.7). The simulation results for different values of k_1 are also shown. Simulation 1, $k_1 = 1.63 \times 10^8$ M $^{-1}$ s^{-1}; Simulation 2, $k_1 = 2.20 \times 10^7$ M $^{-1}$ s^{-1}; Simulation 3, $k_1 = 2.98 \times 10^6$ M $^{-1}$ s^{-1}; Simulation 4, $k_1 = 4.03 \times 10^5$ M $^{-1}$ s^{-1}; Simulation 5, $k_1 = 5.46 \times 10^4$ M $^{-1}$ s^{-1}; Simulation 6, $k_1 = 7.39 \times 10^3$ M $^{-1}$ s^{-1}.

While the featured experiment is based on important assumptions, such as lack of direct reactivity of the reaction intermediates in the oxygen reduction reaction at the tip or substrate, the experiment proves that reactions of an electrogenerated species can be probed, and that a distinguishable signal at the tip can be recorded. An interesting possibility would be that of imaging the surface reactivity by substrate-generated species when the tip size, the resolution required, or the stability of the tip material represent a problem. For instance, it is known that optimal conditions for substrate generation/tip collection imaging in SECM require the spatially compromising use of large tips and values of RG[31,45] as well as stable electrochemical reactions (e.g. many electrode materials exhibit decreasing catalytic properties over time, which results in drifting responses). In the presented mode, the monitoring of a stable tip current, characteristic of the use of a reversible mediator in the feedback mode is achieved, even at longer distances than conventional positive feedback allows.

Conclusions

We have evaluated the use of the scanning electrochemical microscope to carry out a homogeneous chemical reaction at a picoliter volume created in the gap between two SECM probes, and to detect this reaction through the use of the feedback mode. The reactants were electrogenerated, one at each probe, and the feedback signal was expected to yield information about the extent of the reaction. For a first case, called "reversible", the experimental approach curves, both in the case of feedback and annihilation, fit the digital simulation results very well, but the homogenous electron-transfer rate of the reaction between $Fe(CN)_6^{3-}$ and $Ru(NH_3)_6^{2+}$ cannot be discerned. This is attributed to a compensation effect that is supported by the digital simulations and indicates that any gain in feedback from the detection of the homogeneous reaction of the generated species comes with an equal loss of collection.

A second "irreversible" case was introduced to avoid collection complications at the tip. We used Fe^{II}[EDTA] generated from Fe^{III}[EDTA] at a carbon fiber UME that also has sluggish kinetics for the reduction of O_2. Electrogenerated O_2 from the substrate (Pt UME) reacted with Fe^{II}[EDTA] generated at the tip, producing H_2O and regenerating Fe^{III}[EDTA] so as to prove the possibility of assessing homogeneous electron transfer through a distinguishable feedback-like signal at the tip. The results, supported by digital simulations, indicate that only in this irreversible case is it possible to evaluate the homogeneous reaction constant, *k*. An estimation using this model system shows that it is possible to estimate reaction constants over a wide working range of 4 orders of magnitude, from $10^3\ M^{-1}\ s^{-1}$ to $10^7\ M^{-1}\ s^{-1}$, when the tip–substrate gap is 20 μm.

Acknowledgments

We thank the National Science Foundation (CHE-0808927) and the Robert A. Welch Foundation (F-0021) for support of this research. Q. Wang thanks the National Scholarship Fund of the China Scholarship Council for support and research advisor Dr. Huibo Shao from the Beijing Institute of Technology. Helpful discussions with Fu-Ren F. Fan and Cheng-Lan Lin are also gratefully acknowledged. J. Rodríguez-López thanks Eli Lilly & Company for a Division of Analytical Chemistry of the American Chemical Society graduate fellowship; also the complementary scholarship support provided by the Secretaría de Educación Pública of Mexico and the Mexican Government is acknowledged.

Keywords: electrogeneration · electron transfer · feedback · redox chemistry · scanning electrochemical microscopy

[1] *Scanning Electrochemical Microscopy* (Eds.: A. J. Bard, M. V. Mirkin), Marcel Dekker, New York, **2001**.
[2] A. J. Bard, F.- R. F. Fan, J. Kwak, O. Lev, *Anal. Chem.* **1989**, *61*, 132 – 138.
[3] A. J. Bard, F.-R. F. Fan, D. T. Pierce, P. R. Unwin, D. O. Wipf, F. Zhou, *Science* **1991**, *254*, 68 – 74.
[4] A. J. Bard, G. Denuault, C. Lee, D. Mandler, D. O. Wipf, *Acc. Chem. Res.* **1990**, *23*, 357 – 363.
[5] J. Rodríguez-López, M. A. Alpuche-Avilés, A. J. Bard, *J. Am. Chem. Soc.* **2008**, *130*, 16985 – 16995.
[6] Q. Wang, J. Rodríguez-López, A. J. Bard, *J. Am. Chem. Soc.* **2009**, *131*, 17046 – 17047.
[7] J. V. Macpherson, C. J. Slevin, P. R. Unwin, *J. Chem. Soc. Faraday Trans.* **1996**, *92*, 3799 – 3805.
[8] P. R. Unwin, A. J. Bard, *J. Phys. Chem.* **1992**, *96*, 5035 – 5045.
[9] C. J. Slevin, P. R. Unwin, *J. Am. Chem. Soc.* **2000**, *122*, 2597 – 2602.
[10] L. H. Lie, M. V. Mirkin, S. Hakkarainen, A. Houlton, B. R. Horrocks, *J. Electroanal. Chem.* **2007**, *603*, 67 – 80.
[11] D. Mandler, P. R. Unwin, *J. Phys. Chem. B* **2003**, *107*, 407 – 410.
[12] A. P. O'Mullane, J. V. Macpherson, P. R. Unwin, J. Cervera-Montesinos, J. A. Manzanares, F. Frehill, J. G. Vos, *J. Phys. Chem. B* **2004**, *108*, 7219 – 7227.
[13] J. Zhang, C. J. Slevin, C. Morton, P. Scott, D. J. Walton, P. R. Unwin, *J. Phys. Chem. B* **2001**, *105*, 11120 – 11130.
[14] B. Liu, S. A. Rotenberg, M. V. Mirkin, *Anal. Chem.* **2002**, *74*, 6340 – 6348.
[15] J. H. Espenson, *Chemical Kinetics and Reaction Mechanisms, 2nd ed.*, McGraw-Hill, New York, **1995**.
[16] K. J. Laidler, *Chemical Kinetics, 3rd ed.*, Harper & Row, New York, **1987**.
[17] A. J. Bard, L. R. Faulkner, *Electrochemical Methods*, Wiley, New York, **2001**.
[18] R. S. Nicholson, I. Shain, *Anal. Chem.* **1964**, *36*, 706 – 723.
[19] J.-M. Saveant, *Elements of Molecular and Biomolecular Electrochemistry*, Wiley-Interscience, New York, **2006**.
[20] F. Zhou, P. R. Unwin, A. J. Bard, *J. Phys. Chem.* **1992**, *96*, 4917 – 4924.
[21] S. Bollo, L. Nunez-Vergara, J. A. Squella, *J. Electrochem. Soc.* **2004**, *151*, E322 – E325.
[22] S. Bollo, P. Jara-Ulloa, S. Finger, L. J. Nunez-Vergara, J. A. Squella, *J. Electroanal. Chem.* **2005**, *577*, 235 – 242.
[23] Y. Shao, M. V. Mirkin, J. F. Rusling, *J. Phys. Chem. B* **1997**, *101*, 3202 – 3208.
[24] T. Sugihara, T. Kinoshita, S. Aoyagi, Y. Tsujino, T. Osakai, *J. Electroanal. Chem.* **2008**, *612*, 241 – 246.
[25] W. Chang, M. V. Mirkin, A. J. Bard, *J. Phys. Chem.* **1995**, *99*, 16033 – 16042.
[26] J. Ufheil, C. Heb, K. Borgwarth, J. Heinze, *Phys. Chem. Chem. Phys.* **2005**, *7*, 3185 – 3190.
[27] G. Wittstock, W. Schuhmann, *Anal. Chem.* **1997**, *69*, 5059 – 5066.
[28] F.-R. F. Fan, A. J. Bard, *Science* **1995**, *267*, 871 – 874.
[29] P. Sun, M. V. Mirkin, *J. Am. Chem. Soc.* **2008**, *130*, 8241 – 8250.
[30] T. Li, L. Su, W. Hu, H. Dong, Y. Li, L. Mao, *Anal. Chem.* **2010**, *82*, 1521 – 1526.
[31] C. M. Sánchez-Sánchez, J. Rodríguez-López, A. J. Bard, *Anal. Chem.* **2008**, *80*, 3254 – 3260.
[32] S. Seibig, R. van Eldik, *Inorg. Chem.* **1997**, *36*, 4115 – 4120.
[33] V. Zang, R. van Eldik, *Inorg. Chem.* **1990**, *29*, 1705 – 1711.
[34] D. F. Laine, A. Blumenfeld, I. F. Cheng, *Ind. Eng. Chem. Res.* **2008**, *47*, 6502 – 6508.
[35] J. E. Baur, R. M. Wightman, *J. Electroanal. Chem. Interfacial Electrochem.* **1991**, *305*, 73 – 81.
[36] Y. Selzer, I. Turyan, D. Mandler, *J. Phys. Chem. B* **1999**, *103*, 1509 – 1517.
[37] J. Rodríguez-López, M. Shen, A. Nepomnyashchii, A. J. Bard, unpublished results.
[38] C. Amatore, C. Pebay, L. Servant, N. Sojic, S. Szunerits, L. Thouin, *ChemPhysChem* **2006**, *7*, 1322 – 1327.
[39] D. M. Stanbury, O. Haas, H. Taube, *Inorg. Chem.* **1980**, *19*, 518 – 524.
[40] F. C. Anson, C.-L. Ni, J.-M. Saveant, *J. Am. Chem. Soc.* **1985**, *107*, 3442 – 3450.
[41] B. Wang, *J. Power Sources* **2005**, *152*, 1 – 15.
[42] A. P. Purmal, Y. I. Skurlatov, S. O. Travin, *Bull. Acad. Sci. USSR Div. Chem. Sci. (Engl. Transl.)* **1980**, *29*, 315.
[43] J.-P. Randin in *Encyclopedia of Electrochemistry of the Elements, Vol. 7* (Ed.: A. J. Bard), Marcel Dekker, New York, **1976**, pp. 54 – 69.
[44] H. J. Wubs, A. Beenackers, *Ind. Eng. Chem. Res.* **1993**, *32*, 2580 – 2594.
[45] A. Minguzzi, M. A. Alpuche-Aviles, J. Rodríguez-López, S. Rondinini, A. J. Bard, *Anal. Chem.* **2008**, *80*, 4055 – 4064.

Received: March 5, 2010
Published online on August 4, 2010

